THE ASTROPHYSICAL JOURNAL, 309:755–761, 1986 October 15

SMALL-SCALE STRUCTURE OF THE CIRCUMSTELLAR GAS OF HL TAURI AND R MONOCEROTIS

S. BECKWITH,[1,2] AND A. I. SARGENT,[3]

AND

N. Z. SCOVILLE,[3] C. R. MASSON,[3] B. ZUCKERMAN,[4] AND T. G. PHILLIPS[3]

Received 1985 December 16; accepted 1986 April 3

ABSTRACT

Interferometric observations of CO ($J = 1$–0) emission in HL Tau and R Mon reveal small-scale ($\lesssim 6''$) concentrations of molecular gas coincident with both stars. The line widths are small, less than 3 km s^{-1}, and centered close to the stellar velocities, indicating that these condensations are bound to the stars. Lower limits to the circumstellar masses can be derived from the CO measurements and are $\sim 2 \times 10^{-4}$ $M_\odot$ for HL Tau and $\sim 7 \times 10^{-3}$ $M_\odot$ for R Mon. HL Tau is also a source of 2.7 mm continuum radiation, which probably originates from dust near the star. Depending upon the dust emissivity law adopted, the continuum flux implies a total mass of gas and dust of 1×10^{-2} to 2×10^{-1} $M_\odot$. These results, combined with near infrared speckle interferometry, suggest that both stars are embedded in disks with sizes and masses similar to those of the primitive solar nebula.

Subject headings: stars: circumstellar shells — stars: individual — stars: pre–main sequence

I. INTRODUCTION

Circumstellar matter almost certainly plays a crucial role in the condensation and early evolution of stars. It has been postulated that, in the earliest stages of star formation, this material resides in viscous disks which may be instrumental in dissipating angular momentum and magnetic fields (e.g., Spitzer 1978). Perhaps the most interesting phase occurs quite late in the evolution of protostars, when planetary or close binary systems may be created from the surrounding matter (Hartmann 1978 and references therein; Harrington 1982; Abt and Levy 1976).

As yet, very few direct observations of the material within a few hundred AU of the youngest stars exist, primarily because angular resolutions of a few seconds of arc or better are required. Several recent studies have shown, however, that significant quantities of material remain associated with stars long after nuclear ignition (Aumann 1984; Aumann *et al.* 1984; Smith and Terrile 1984; Hobbs *et al.* 1985).

Molecular line observations of several young stars suggest the presence of disklike, circumstellar structures (e.g., Plambeck *et al.* 1982; Cantó *et al.* 1983; Kaifu *et al.* 1984; Scoville *et al.* 1986), but on spatial scales of a few thousand AU or more, probably too large to be important for planet formation. Higher resolution observations of scattered infrared light near the stars HL Tau and R Mon (Beckwith *et al.* 1984; Grasdalen *et al.* 1984) indicate disks of dust on spatial scales of a few hundred AU. If gas and dust coexist in the ratio typical of the galactic interstellar medium, the sizes and masses of the HL Tau and R Mon disks are comparable to the present-day size and mass of the solar planetary system. To detect gas on these scales, molecular line measurements at comparably high angular resolution are required.

In this paper, we present observations made with the Owens Valley millimeter-wave interferometer of both the $J = 1$–0 CO line emission and the continuum radiation at 112 GHz near HL Tau and R Mon, at distances of 160 pc (Kuhi 1964) and 800 pc (Walker 1956), respectively. These measurements are sensitive probes of the total mass, distribution, and velocity field of the circumstellar gas at resolution similar to that obtained with infrared and optical imaging techniques. Since the interferometer also resolves out relatively smooth, large-scale emission, it is possible to study structures on scales of only a few hundred AU at the distances of these objects. The observations described below constitute the first high spatial resolution study of the cool gas around young stellar objects.

II. OBSERVATIONS

The observations were made using the three-element millimeter wave interferometer at the Owens Valley Radio Observatory (Masson *et al.* 1985) between April and July 1984. Five separate configurations of the three 10.4 m telescopes were used. Unprojected baselines varied from 14 to 60 m. The resulting synthesized beam widths were $10\overset{''}{.}5 \times 6\overset{''}{.}0$ at P.A. $1\overset{\circ}{.}7$, for HL Tau, and $11\overset{''}{.}1 \times 5\overset{''}{.}8$ at P.A. $4\overset{\circ}{.}7$, for R Mon. The primary beam size was $\sim 65''$.

Each telescope is equipped with a cooled SIS receiver (Woody, Miller, and Wengler 1985), which operated double sideband so that the interferometer was sensitive to two frequency bands; the signals were separated and recorded independently. For the observations described here, the frequency of the CO $J = 1$–0 transition was centered in the upper sideband; continuum emission at $\lambda = 2.7$ mm was observed from the lower sideband using a filter with 200 MHz bandpass. For the CO measurements, a filterbank of 32×1 MHz channels provided velocity coverage of 83 km s^{-1} with resolution of 2.6 km s^{-1}.

Phase calibration was carried out by measuring standard point sources every half hour; the calibrators were 0420−01 and 0528+134 for HL Tau and R Mon, respectively. Positional uncertainty as a result of errors in baseline determinations and phase calibration is $\sim 2''$. Corrections for atmospheric attenuation and receiver gain changes were made

[1] Department of Astronomy, Cornell University.
[2] Alfred P. Sloan Fellow.
[3] Division of Physics, Mathematics, and Astronomy, California Institute of Technology.
[4] Department of Astronomy, University of California–Los Angeles.

using standard chopper wheel techniques. Daily measurements of W3(OH) (4.0 Jy) and of Uranus ($T_B = 134$ K; Ulich 1981) established the flux density scale. Uncertainties in the absolute fluxes are $\sim 20\%$. Following calibration of the data, images were created and cleaned using the NRAO AIPS package.

III. RESULTS

In § III*a*, we present and discuss maps of the CO emission in the central velocity channels for HL Tau and R Mon. Continuum emission was also seen toward HL Tau and is described in § III*b*. No continuum emission was seen toward R Mon to a limit of 60 mJy (3 σ).

a) CO Line Radiation

Figures 1 and 2 display maps of the CO emission in the central few velocity channels for HL Tau and R Mon, respectively. Crosses mark the stellar positions (Jones and Herbig 1979, 1982; Cohen and Schwartz 1983). There is no evidence of CO emission, to a limit of 1 K (3 σ) in antenna temperature, in the maps of the other channels. To within the positional uncertainties, significant CO peaks coincide with the stars. Furthermore, the line velocities are very close to the stellar velocities inferred from optical spectra (e.g., Herbig and Rao 1972) and to the nearby cloud velocities seen in single-dish CO spectra (Edwards and Snell 1982; Calvet, Cantó, and Rodríguez 1983).

The peak flux densities for the CO emission toward HL Tau and R Mon are 3.8 and 4.9 Jy, respectively, corresponding to brightness temperatures of 5.4 and 7.0 K. These enhancements are comparable to the mean brightness of the larger molecular clouds against which the stars are seen; single-dish observations of both objects indicate brightness temperatures ~ 8 K in 65″ beams, implying relatively uniform emission over areas 100 times larger than the source sizes in Figures 1 and 2. The interferometer has effectively resolved out this extended emission to reveal the smaller sources coincident with the stars.

These emission peaks correspond to enhanced column density of CO near the star, if the line is optically thin, or to enhanced excitation temperature, if the line is optically thick. In either case, it is evident that the CO emission reflects the presence of gaseous halos around HL Tau and R Mon. The spatial resolution attainable with the radio interferometer, $\sim 6''$, is as yet insufficient to determine the precise morphology, but we tentatively identify this gas with that inferred from the infrared observations (Beckwith *et al.* 1984; Grasdalen *et al.* 1984), which reveal the presence of dust halos $\sim 2''$ across.

The maps of R Mon shown in Figure 2 have at least two components. The central core is not completely unresolved but exhibits slight enhancements along northeast and northwest lines. In addition, there is a separate extension, ~ 3 σ above the noise, lying along a northeast line outside the core. Figure 3 (Plate 10) shows the CO contours of the central channel superposed on a photograph of the nebula, kindly provided by Dr. T. Neckel. It can be seen from this figure that the extension, which appears only in the central velocity channel, is coincident with the eastern optical edge of the nebulosity north of R Mon, NGC 2261, known as Hubble's variable nebula. It may be that both this extension and the enhancements in the core source correspond to increases in CO column density along

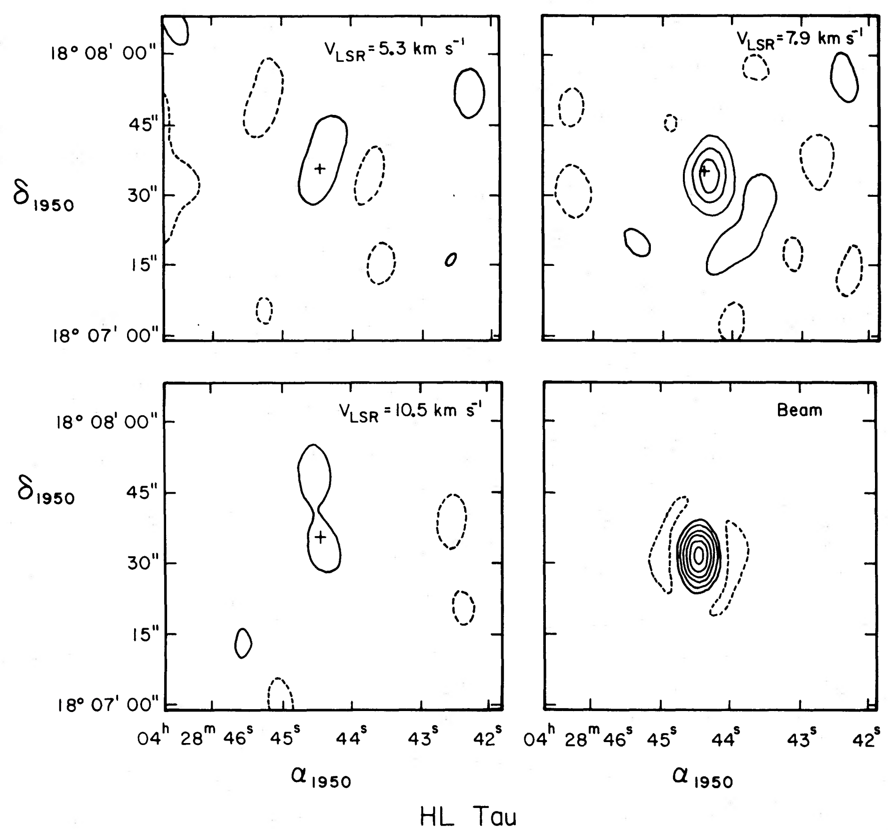

FIG. 1.—Maps of the central three channels of CO emission and the synthesized beam toward HL Tau. Contours are spaced by 1 Jy per beam, and the lowest contour is at the 1 Jy level. The peak flux density in the 7.9 km s^{-1} channel is 3.8 Jy. In each channel map, a cross marks the optical position of the star. There was no evidence for emission above the noise level in maps of any of the other 32 channels.

1986ApJ...309..755B

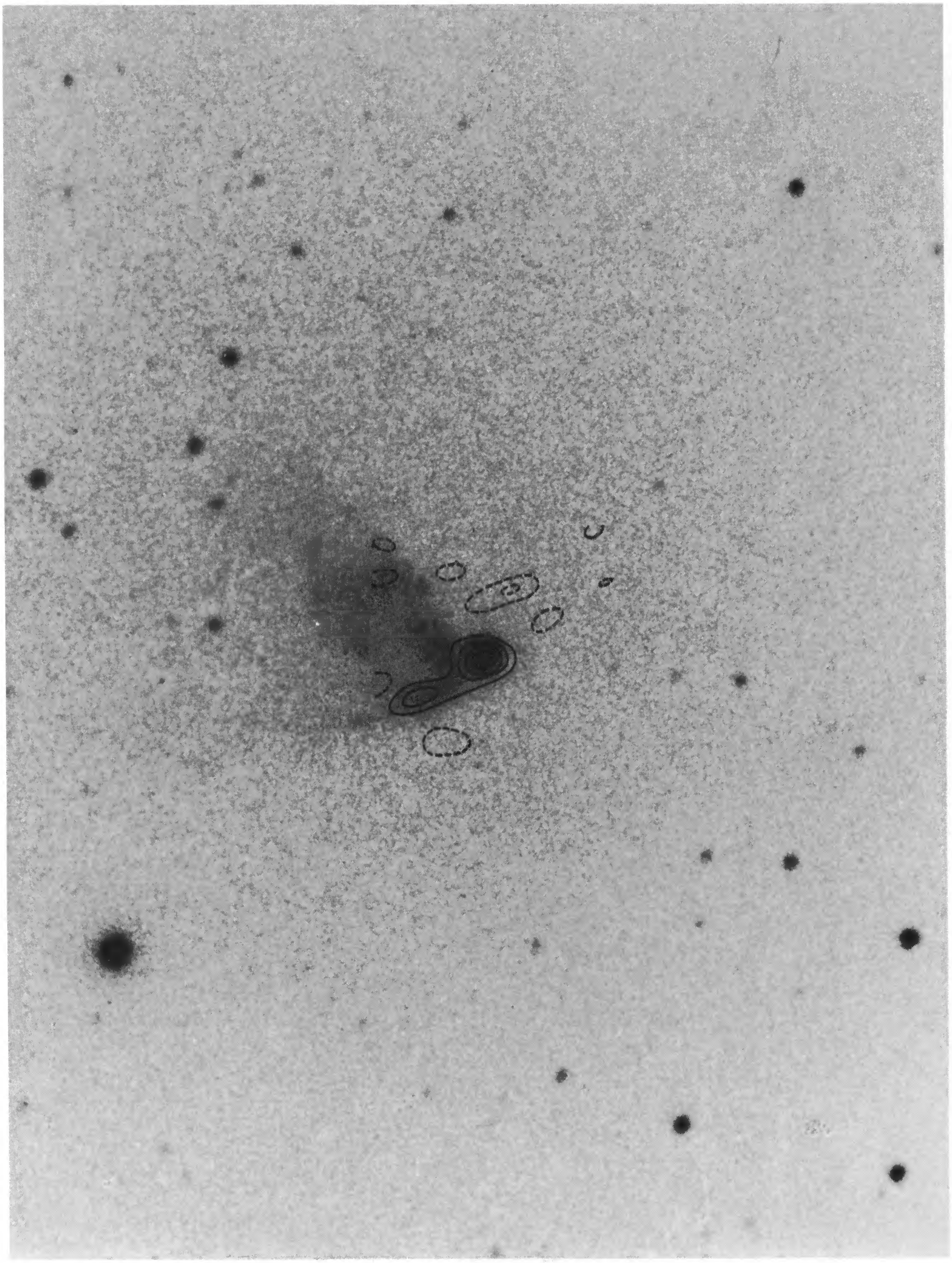

FIG. 3.—CO contours from the central velocity channel superposed on a photograph of R Mon. The photograph is from an S1 image tube plate taken by T. Neckel of the Max-Plank-Institut für Astronomie. It has an effective wavelength in the near infrared of ~8000 Å.

BECKWITH *et al.* (*see* page 756)

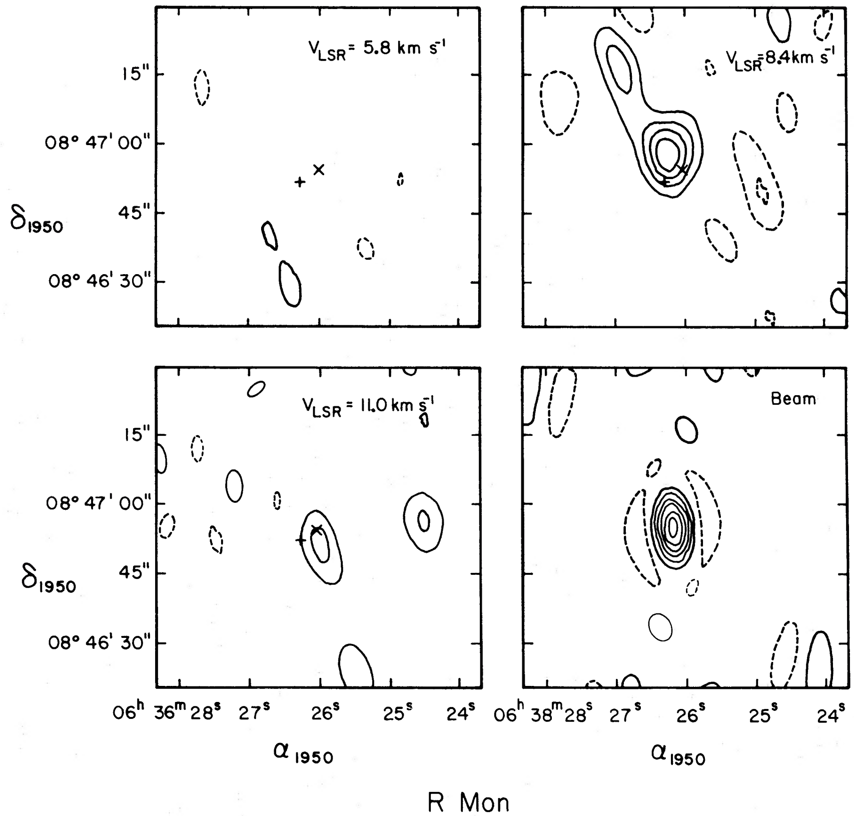

FIG. 2.—Maps of the central channels of CO emission toward R Mon, together with the synthesized beam. The contour levels are the same as in Fig. 1 and the peak flux density in the 8.4 km s^{-1} channel is 4.9 Jy. No other velocity channels showed evidence for CO emission. A plus sign (+) marks the infrared position of the star (see Cohen and Schwartz 1983), and a cross (×) marks the position of the base of NGC 2261.

the edges of the nebula, where gas swept up by the outflow from R Mon is channeled north into the optical nebulosity (Cantó *et al.* 1982; Jones and Herbig 1982).

Figure 1 shows that in HL Tau the CO emission region is also at least partially unresolved. From the single observation of an unresolved CO line, it is impossible to specify uniquely the optical depth, excitation temperature, and source size. However, from a judicious choice of the temperature, we may derive good lower limits to the mass of gas and to the size of the gaseous halo. The brightness temperature, T_B, and the optical depth, τ, at the CO line center are given by (see Scoville *et al.* 1986, and references therein)

$$T_B = \frac{\Omega_s}{\Omega_B} T_X(1 - e^{-\tau}) \tag{1}$$

and

$$\tau \approx \frac{7.5 \times 10^{-16}}{\Delta v} \left(\frac{T_0}{T_X}\right)^2 N_{\rm CO} . \tag{2}$$

The quantities Ω_s and Ω_B are the source and beam solid angles, respectively, T_X is the level excitation temperature, $T_0 = h\nu/k = 5.5$ K, Δv is the FWHM of the line (km s^{-1}), and $N_{\rm CO}$ the column density of CO (cm^{-2}). On the basis of the maps, Δv is assumed to be 2.6 km s^{-1}, although its value is unimportant for the derivation of the mass if the emission is optically thin. For optically thin emission, the brightness temperature $T_B \approx (\Omega_s/\Omega_B)T_X\tau$ and the halo mass (in grams) in terms of the observed brightness temperature and the excitation temperature is then

$$M_h = 3.5 \times 10^{27}\left(\frac{\Omega_B D^2}{\xi}\right)T_B T_X , \tag{3}$$

where ξ is the fractional CO abundance, D is the source distance in pc, and Ω_B is 1.7×10^{-9} sr for both HL Tau and R Mon. If the source size is much smaller than the beam, however, the column density can be underestimated. Equation (3) provides a firm lower limit to the mass, if the excitation temperature is known.

Although T_X cannot be determined uniquely from the observations, it is quite likely to be close to the dust temperature near the stars. As described in § III*b*, typical interstellar grains with long wavelength emissivities proportional to λ^{-1} (e.g., Hildebrand 1983) will be at $\sim$35–70 K within projected radii of $\sim 2''.5$ from either star, the larger distance to R Mon being compensated by its larger luminosity (e.g., Cohen *et al.* 1983). Assuming the emission is optically thin, and taking $T_X = 50$ K and $\xi = 10^{-4}$, lower limits to the halo masses are, respectively, $\sim 4 \times 10^{29}$ g ($2 \times 10^{-4}\ M_\odot$) and $\sim 1.3 \times 10^{31}$ g ($7 \times 10^{-3}\ M_\odot$). These are approximations, since T_X and ξ may be different by factors of order 2. Since we believe the CO is optically thick (see § IV), the halo masses are in any case larger than these estimates by a factor $\sim \tau$.

For optically thick lines, the ratio of the observed, beam-averaged, brightness temperature to the assumed excitation temperature yields the beam filling factor and thus the source size. For $T_X = 50$ K, the source solid angles for both HL Tau and R Mon would have to be at least $\sim 2 \times 10^{-10}$ sr, corresponding to regions $\sim 3''$ or larger in diameter. Since they appear unresolved in the $\sim 6''$ beams, the sources are less than $\sim 6''$ across. They are comparable to the $\sim 2''$ diameter regions responsible for the scattered infrared light seen at near infrared wavelengths (Beckwith *et al.* 1984; Grasdalen *et al.* 1984). The corresponding linear radii are 250 AU and 1200 AU for HL Tau and R Mon, respectively.

b) Continuum Radiation

Figure 4, the map of the 112 GHz continuum emission from HL Tau, shows an unresolved continuum source spatially coincident with the star and, by implication, with the line emission. The flux density is 100 mJy, a 5 σ detection. Continuum emission at 2.7 mm from a T Tauri star most likely results from free-free radiation in ionized gas or thermal emission from dust.

Free-free emission is detected around many pre–main sequence stars. The flux density for free-free radiation scales as ν^{α} with $\alpha \leq 2$, depending on the density gradient and optical depth (e.g., Wright and Barlow 1975; Panagia and Felli 1975; Simon *et al.* 1983). Cohen, Bieging, and Schwartz (1982) place an upper limit of 160 μJy on the 6 mm flux density from HL Tau with a $0\overset{''}{.}1$ beam. Brown, Mundt, and Drake (1985) detect 6 cm emission, over $\sim 10''$ in extent, near HL Tau with peak flux density 250 μJy $\approx 3''$ west of the star. For the extreme case $\alpha = 2$, this implies that the 2.7 mm emission should be less than 130 mJy, consistent with the present observations. But a spectral index $\alpha = 2$ corresponds to the case of an optically thick H II region, and if the typical source temperature is ~ 7000 K, then the H II region must be $0\overset{''}{.}16$ across, much smaller than the extended region observed to the west. It is unlikely that the 2.7 mm continuum radiation is associated with this emission.

Observations of the Brα and Brγ lines of H II at 4.05 and 2.16 μm place stronger limits on the free-free component. Persson *et al.* (1984) observed a Brα line flux from HL Tau of 8×10^{-13} ergs s^{-1} cm^{-2}, a value confirmed by our own unpublished

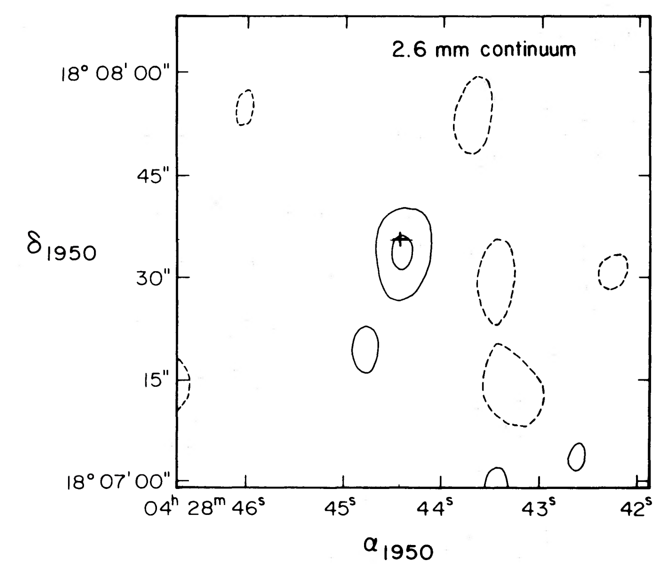

FIG. 4.—A map of the 2.6 mm continuum emission toward HL Tau. The peak flux density is 0.10 Jy with a significance of ~ 5 σ. Contour levels are at 0.04 Jy per beam.

observations with an $8''$ beam (Evans *et al.* 1986). Assuming optically thin emission, the ratio of the 2.7 mm continuum flux density to Brα flux is 2.8×10^{-13} Hz^{-1} (see Wynn-Williams 1982), implying a 2.7 mm flux density of 22 mJy. Since large optical depths always reduce this ratio, this represents an upper limit to the flux density of the 2.7 mm free-free component, considerably less than the observed value of 100 mJy. Thus, the continuum emission must arise from dust, not in ionized gas.

Figure 5 presents the spectrum of HL Tau between infrared and radio frequencies, along with curves showing the emission spectra of gray particles and of particles whose radiative cross section increases linearly with frequency. It is evident that emission by gray particles is just consistent with the 160 μJy upper limit at 6 cm. The fluxes reported between 50 and 200 μm are somewhat larger than expected from an extrapolation from our 2.7 mm observation. However, these far infrared observations were carried out with a much larger beam, $45''$, and may include emission from a more extended area of the circumstellar cloud than was indicated in the 2.7 mm measurement. Furthermore, the figure indicates only statistical uncertainties; other discrepancies between the infrared and millimeter flux densities can arise from the different calibration procedures employed. It is therefore possible that the 2.7 mm continuum flux in the HL Tau environment includes a substantial contribution from large particles which are not commonly seen in the interstellar medium. Cohen (1983) also noted this possibility in his analysis of the amount of dust needed to produce the far-infrared continuum emission.

Dust continuum emission is usually characterized as $Q_\nu B_\nu(T)$, where Q_ν is the effective dust emission cross section, and $B_\nu(T)$ is the blackbody function. Since $Q_\nu \approx \nu^\beta$ with $\beta \gtrsim 1$ for small particles, and $B_\nu(T) \approx \nu^2$ at millimeter wavelengths, our observed 2.7 mm flux density is entirely consistent with the 6 cm upper limit of 160 μJy. As we will demonstrate, the amount of dust necessary to produce detectable levels of continuum radiation at this wavelength is relatively small, making it reasonable to interpret the continuum flux as arising from solid particles.

Hildebrand (1983) has derived a relation between the long wavelength flux density from dust and the total mass of hydrogen for typical interstellar conditions. Taking F_ν as the flux density and T_d as the dust temperature, the mass of gas M_g is,

$$M_g = C \frac{F_\nu D^2}{B_\nu(T_d)} \approx C \frac{F_\nu D^2 \lambda^2}{2kT_d} . \tag{4}$$

The constant C is derived empirically from dark cloud observations; it has a typical value of $10(\lambda/250\ \mu\mathrm{m})^\beta$ g cm^{-2}.

For a dust grain at distance r from a source of luminosity L_* and effective temperature T_e, equilibrium between the absorbed light and the reemitted thermal radiation determines the dust temperature (see Spitzer 1978). If the same spectral dependence for the emission and absorption cross sections of the dust grains is assumed, then the grain temperature is

$$T_d = \left(\frac{L_* T_e^\beta}{16\pi\sigma r^2}\right)^{1/(4+\beta)} , \tag{5}$$

where σ is the Stefan-Boltzmann constant. Thus T_d can be accurately determined, if T_e is known approximately.

For HL Tau, $L_* = 7.2\ L_\odot$ (Cohen 1983). The effective temperature of the radiation field heating the dust a few hundred AU from the star depends on the amount of radiative transfer

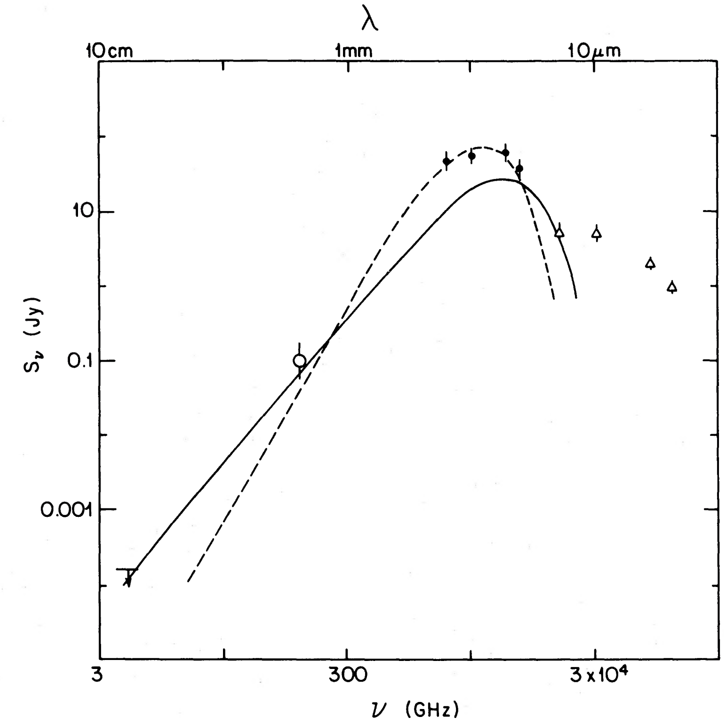

FIG. 5.—A spectrum of HL Tau made by combining observations of Cohen (1983; *filled circles*), Cohen, Bieging, and Schwartz (1982; upper limit at 6 GHz), and this paper (open circle). The figure displays only statistical uncertainties; the (unknown) calibration errors are likely to be comparable. Note that the far-infrared fluxes were measured with a 45″ beam, considerably larger than that at any other wavelengths. The solid line shows a blackbody adjusted to fit the long wavelength data; the dashed line shows a blackbody modified by a λ^{-1} emissivity, as appropriate for the emission from small particles at shorter wavelengths.

provided by dust at small radii. The two extreme cases are $T_e = 4000$ K, the effective temperature of the star itself, and $T_e \approx 60$ K, the temperature of the radiation field observed at Earth. At the adopted distance of 160 pc, grains located at 2″ from the star will have $T_d \approx 25$ K ($\beta = 0$), 35–71 K ($\beta = 1$), or 59–135 K ($\beta = 2$), where the ranges result from the uncertain T_e. The choice of 50 K for the gas temperature in § III*a* is likely to be within a factor of 2 of the actual temperature even in the most extreme cases, if the gas and dust temperatures are reasonably well coupled. Using the median temperature characterizing particles with different β, equation (3) gives a total mass of $\sim 2 \times 10^{31}$ g ($\beta = 0$), 1×10^{32} g ($\beta = 1$), and 7×10^{32} g ($\beta = 2$). If most of the mass is in large particles, the continuum flux implies a circumstellar mass of $\sim 0.01\ M_\odot$.

IV. DISCUSSION

Whether the CO lines are optically thick or thin, it is evident from these observations, together with the results of speckle interferometry (Beckwith *et al.* 1984), that the gas densities must increase sharply at the positions of the stars HL Tau and R Mon. This gas may be bound to the stars by the stellar gravity and confined in Keplerian orbits. Alternatively, it may result from mass outflow, as in the case of evolved stars (Zuckerman 1980). From the morphology, it is impossible to distinguish between these possibilities.

Both stars are known to be losing mass (Jones and Herbig 1982; Cantó *et al.* 1982; Edwards and Snell 1982; Calvet, Cantó, and Rodríguez 1983). The individual maps clearly show almost all the emission at the central velocity, however, and the velocity range of the gas does not exceed ~ 3 km s^{-1}. Even the jetlike extension in the R Mon map is confined to a single channel at the velocity of the more extended molecular cloud. The small line widths of the CO make it unlikely that the CO peaks result from mass loss by the stars. Outflow from HL Tau, for example, creates lines in the larger molecular cloud with widths greater than 5 km s^{-1} and wings extending to more than 10 km s^{-1} (Calvet, Cantó, and Rodríguez 1983; Edwards and Snell 1982).

We argue, therefore, that the CO detected by the interferometer arises from relatively stationary gas confined by the gravitational pull of the stars. The close spatial correspondence of the CO emission with the stellar positions and velocities suggests this is gas associated with the dust seen at infrared wavelengths. In HL Tau, the near-infrared data (Beckwith *et al.* 1984) show a halo, 2″ across, with a total mass greater than $\sim 2 \times 10^{-4}\ M_\odot$, whereas the CO data imply at least $2 \times 10^{-4}\ M_\odot$ in a region $\sim$3″–6″ in diameter. The near-infrared data for R Mon give a size $\sim$1″.6 and mass more than $3 \times 10^{-3}\ M_\odot$, similar to the 3″–6″ and $7 \times 10^{-3}\ M_\odot$ found in this paper. The most straightforward interpretation is that the gas and dust orbit the stars and are possibly confined to disks.

A. SOURCE MORPHOLOGY

Assuming HL Tau is a 1 $M_\odot$ star, the velocity of material in circular orbits can be expressed as a function of distance from the star as

$$v(r) = \left(\frac{GM_*}{r}\right)^{1/2} = 2.4\alpha_{160}^{-1/2}\ \mathrm{km\ s^{-1}}\ , \tag{6}$$

where α_{160} is the angular radius in seconds of arc at 160 pc. The projected velocity of the bulk of the material is ~ 1.3 km s^{-1} or less, implying angular radii $\sim 3''$ or greater. If the gas is in a disk tilted along the line of sight, the angular radius may be smaller. This size is similar to the size of the CO source, 1″.5 ≤ $\alpha_{CO} \lesssim$ 2″.5, depending on the optical depth and orientation of the disk with respect to the beam.

The situation is less clear cut for R Mon, where velocity information provides little constraint on the source size. R Monocerotis is 5 times more distant than HL Tau, but the star is more massive, perhaps as much as 5 $M_{\odot}$. Since emission is present in two velocity channels (albeit very weakly in one), the line width is 3–5 km s^{-1}, and it is easy to make a disk model consistent with the observations. As in HL Tau, the data support the interpretation that R Mon is surrounded by a relatively massive gaseous halo, possibly orbiting the star.

b) Disk Masses

The mass of gas associated with the HL Tau halo has been determined in three independent ways. The lower limit to the column density of CO implies a lower limit to the mass of H_2, presumably the main constituent, of 2×10^{-4} $M_{\odot}$. A second lower limit of 2×10^{-4} $M_{\odot}$ is based on the fraction of scattered light at 2.2 μm (Beckwith *et al.* 1984). These limits are considerably smaller than the estimate of $\sim 10^{-2}$ $M_{\odot}$ based on the assumption that dust particles are responsible for the 2.7 mm continuum radiation, but they are all consistent if the CO emission and near-infrared scattering regions are optically thick and the actual mass is closest to that implied by 2.7 mm continuum. Optically thick CO occurs commonly in the interstellar medium, whereas a gas/dust ratio of much less than 100 by mass has never been observed unambiguously. We therefore favor the point of view that the CO is optically thick.

Each of the above observational techniques probes a different aspect of the circumstellar matter distribution. Although both the near-infrared scattered light and 2.7 mm continuum trace the solid material, the bulk of the near-infrared scattering probably results from micron-sized particles in regions subtending large solid angles as seen from the stars, such as the outer portions of very thick disks. The 2.7 mm continuum, on the other hand, may be produced by a range of particle sizes from microns to millimeters and is relatively insensitive to the particle size and spatial distribution. Thus, if there is substantial mass in the inner regions of very thin disks, these can be more easily studied via millimeter continuum and line emission.

For HL Tau, the circumstellar mass is of order 0.01 $M_{\odot}$. This is approximately equal to the "minimum" mass for the solar nebula prior to the formation of the planets in the solar system (Weidenschilling 1977; Cassen and Moosman 1982). Thus, HL Tau may be in an early stage of planetary formation very similar to that which occurred in the solar nebula.

The lower limit to the gas mass around R Mon from CO data is 7×10^{-3} $M_{\odot}$, which is comparable to the 3×10^{-3} $M_{\odot}$ inferred from the scattered light observations. As in HL Tau, the actual mass could be much larger, if the CO is optically thick. The halo in R Mon is considerably larger than the nebula proposed for models of the early solar system but, in both objects, the sizes derived from the near infrared scattered light and the CO emission are similar to that of the disk in β Pic (Smith and Terrile 1985).

Beckwith *et al.* (1984) suggested that the minimum masses and sizes for the dust halos are sufficient to stabilize them against disruption by mass loss from the stars, if the mass ratio of gas to dust is 100. The interferometer data show there is at least this much gas. Unless mass loss from these stars increases by several orders of magnitude, an unlikely occurence considering the generally small mass loss rates among larger samples of T Tauri stars, the circumstellar material should remain in orbit around the stars as they evolve to the main sequence, thus satisfying the first prerequisite for subsequent planet formation.

V. CONCLUSIONS

Millimeter wave interferometric observations reveal small clouds of gas and dust, a few hundred AU in extent, coincident in position and velocity with the stars HL Tau and R Mon. These clouds have sufficiently small velocity dispersions to be bound to the stars and sufficiently high masses to be stable against disruption by stellar winds and radiation pressure. They probably represent residual matter from star formation trapped in the circumstellar environs by stellar gravity.

The sizes of both clouds and the mass of that associated with HL Tau are similar to those attributed to the primitive solar nebula before the planetary system formed. There is some evidence that large particles, of order one millimeter in size, have begun to form, strengthening the analogy with the early solar system.

It is a pleasure to thank S. L. Scott and D. P. Woody for unstinting assistance at the interferometer and R. E. Miller of Bell Laboratories for providing SIS junctions used in the receivers. We are grateful to R. Hildebrand, B. F. Jones, and R. Mundt for enlightening discussions. M. F. Skrutskie provided image processing software contributing to this work, while M. Sarcander and T. Neckel generously donated their time and an infrared plate of R Mon to make Figure 5. Partial support for this research was provided by the NSF through grants AST-8412473, AST-8403054, AST 83-18342, and by the Sloan Foundation.

REFERENCES

Abt, H. A., and Levy, S. G. 1976, *Ap. J. Suppl.*, **30**, 273.
Aumann, H. H. 1984, *Bull. A.A.S.*, **16**, 483.
Aumann, H. H., Gillett, F. C., Beichman, C. A., de Jong, T., Houck, J. R., Low, F. J., Neugebauer, G., Walker, R. G., and Wesselius, P. R. 1984, *Ap. J. (Letters)*, **278**, L23.
Beckwith, S., Zuckerman, B., Skrutskie, M. F., and Dyck, H. M. 1984, *Ap. J.*, **287**, 793.
Brown, A., Mundt, R., and Drake, S. A. 1985, in *Radio Stars*, ed. R. M. Hlellming and D. M. Gibson (Dordrecht: Reidel), p. 105.
Calvet, N., Cantó, J., and Rodríguez, L. F. 1983, *Ap. J.*, **268**, 739.
Cantó, J., Rodríguez, L. F., Barral, J. F., and Carral, P. 1981, *Ap. J.*, **244**, 102.
Cassen, P., and Moosman, A. 1981, *Icarus*, **48**, 353.
Cohen, M. 1983, *Ap. J. (Letters)*, **270**, L69.
Cohen, M., Bieging, J. H., and Schwartz, P. R. 1982, *Ap. J.*, **253**, 707.
Cohen, M., Harvey, P. M., Schwartz, R. D., and Wilking, B. A. 1983, *Ap. J.*, **278**, 671.
Cohen, M., and Schwartz, P. R., 1983, *Ap. J.*, **265**, 877.
Edwards, S., and Snell, R. L. 1982, *Ap. J.*, **261**, 151.
Evans, N. J., II, Levreault, R. M., Beckwith, S., and Skrutskie, M. F. 1986, in preparation.
Grasdalen, G. L., Strom, S. E., Strom, K. M., Capps, R. W., Thompson, D., and Castelaz, M. 1984, *Ap. J. (Letters)*, **283**, L57.
Harrington, J. P., 1982, in *Extraterrestrials—Where Are They?*, ed. M. H. Hart and B. Zuckerman (New York: Pergamon Press), p. 142.
Hartmann, W. K., 1978, in *Protostars and Planets*, ed. T. Gehrels (Tucson: University of Arizona Press), p. 58.
Herbig, G. H., and Rao, N. K. 1972, *Ap. J.*, **174**, 401.
Hildebrand, R. H., 1983, *Quart. J.R.A.S.*, **24**, 267.
Hobbs, L. M., Vidal-Madjar, A., Ferlet, R., Albert, C. E., and Gry, C. 1985, *Ap. J. (Letters)*, **293**, L29.
Jones, B. F., and Herbig, G. H., 1979, *A.J.*, **84**, 1872.
———. 1982, *A.J.*, **87**, 1223.
Kaifu, N., *et al.* 1984, *Astr. Ap.*, **134**, 7.

Kuhi, L. V. 1964, *Ap. J.*, **140**, 1409.
Masson, C. R., *et al.* 1985, in *U.R.S.I. Symposium on Millimeter and Submillimeter Wave Astronomy* (Granada: U.R.S.I.), p. 65.
Panagia, N., and Felli, M. 1975, *Astr. Ap.*, **39**, 1.
Persson, S. E., Geballe, T. R., McGregor, P. J., Edwards, S., and Lonsdale, C. J. 1984, *Ap. J.*, **286**, 289.
Plambeck, R. L., Wright, M. C. H., Welch, W. J., Bieging, J. H., Baud, B., Ho, P. T. P., and Vogel, S. N. 1982, *Ap. J.*, **259**, 617.
Scoville, N. Z., Sargent, A. I., Sanders, D. B., Claussen, M. J., Masson, C. R., Lo, K. Y., and Phillips, T. G. 1986, *Ap. J.*, **303**, 416.
Simon, M., Felli, M., Cassar, L., Fischer, J., and Massi, M. 1983, *Ap. J.*, **266**, 623.
Smith, B. A., and Terrile, R. J., 1984, *Science*, **226**, 1421.
Spitzer, L. Jr. 1978, *Physical Processes in the Interstellar Medium* (New York: Wiley).
Ulich, B. L. 1981, *A.J.*, **86**, 1619.
Walker, M. F. 1956, *Ap. J. Suppl.*, **2**, 365.
Weidenschilling, S. J. 1977, *Astr. Space Sci.*, **51**, 153.
Woody, D. P., Miller, R. E., and Wengler, M. J. 1985, *I.E.E.E. Trans.*, **MTT-33**, 90.
Wright, A. E., and Barlow, M. J. 1975, *M.N.R.A.S.*, **170**, 41.
Wynn-Williams, C. G. 1982, *Ann. Rev. Astr. Ap.*, **20**, 597.
Zuckerman, B. 1980, *Ann. Rev. Astr. Ap.*, **18**, 263.

S. Beckwith: Astronomy Department, Cornell University, Space Science Building, Ithaca, NY 14853

C. R. Masson, T. G. Phillips, and A. I. Sargent: Physics, Mathematics, and Astronomy, Downs Laboratory 320-47, California Institute of Technology, Pasadena, CA 91125

N. Z. Scoville: Physics, Mathematics, and Astronomy, Robinson 105-24, California Institute of Technology, Pasadena, CA 91125

B. Zuckerman: Department of Astronomy, University of California Los Angeles, Los Angeles, CA 90024